



Original Article

Application of wavefront reinforcement model for reduction blast-induced ground vibration

Pirat Jaroopattanon^{1*}, Ormsin Indarid¹, and Pham Van Hoa²

¹ Department of Mining and Petroleum Engineering, Faculty of Engineering,
Chiang Mai University, Mueang, Chiang Mai, 50200 Thailand

² Department of Surface Mining, Hanoi University of Mining and Geology, Hanoi, Viet Nam

Received: 18 September 2016; Revised: 17 December 2016; Accepted: 14 January 2017

Abstract

Ground vibration from blasting is generally controlled by reducing the explosive charge weight per delay. However, lowering explosive charge weight per delay may increase the fragmentation size of blasted material. Richards (2008) introduced a wavefront reinforcement model to account for input burden, spacing and sequential delay timing for each blasthole. This study tested his wavefront reinforcement model with a predetermined surface wave velocity at 350 m/s to determine the direction and extent of increases in ground transmitted vibrations. The results from 21 experimental blasts on overburden material (Red Beds) at various patterns and delay timing at Mae Moh Mine indicated that ground vibrations were higher in areas of wavefront reinforcement compared to non-wavefront reinforcement in 16 (76%) of the experimental blasts. The designed drilling patterns and sequential initiation has shown that the wavefront reinforcement areas mainly occur in front and to the back of the blasting direction.

Keywords: wavefront reinforcement model, ground vibration, particle velocity, shear surface wave, Mae Moh Mine

1. Introduction

The Mae Moh Mine operates at Thailand's largest coal deposit. It is situated in the Mae Moh Basin in the Mae Moh District of Lampang Province, about 26 kilometers east of Lampang City. The mine covers an area of about 135 square kilometers, roughly 7 kilometers in an east-west direction and 16 kilometers in a north-south direction. The tertiary sediments of the basin are referred to as the Mae Moh Group. The geological detail of Mae Moh formations including the overburden "Red Bed" can be found in many research papers, such as Songtham *et al.* (2005), Ratanasthien *et al.* (2008), Mavong *et al.* (2014), and Geotechnical Report Mae Moh Mine (1985).

Many research papers had been conducted to predict and reduce blast induced vibration. Shi and Chen (2011)

investigated and established a relationship between peak particle velocity (PPV) and scaled distance (SD) factor proposed by United States Bureau of Mines (USBM). Sixty-six blasts were conducted at the pyrite open-pit mine in China. Maximum charge amount per delay and 15 ms delay were proposed for this mine, and a decrease in vibration intensity of 24.5% was claimed. Similar studies of establishing the relationship between peak particle velocity (PPV) and scaled distance (SD) factor were conducted by Dogan *et al.* (2013), Rachpech *et al.* (2014), Kahrman (2004), and Ozer *et al.* (2008). However, Yan *et al.* (2013) proposed a different mathematical tool involved Bayesian technique and Monte Carlo simulation to shed light on the reliability of the empirical design, two fitting parameters like PPV and scaled distance equation. Hasanipanah *et al.* (2015) introduced and compared a support vector machine (SVM) to empirical equations to predict ground vibration in blasting operations of Bakhtiari Dam, Iran. The results indicated that the SVM method provided higher performance capacity in predicting PPV compared to empirical equations.

*Corresponding author

Email address: pirat@eng.cmu.ac.th

In addition, air deck technique and stem plug were also studied and may be applied to reduce the ground vibration. Such studies were Lheewijit *et al.* (2012), Boonnumma and Leelasukseree (2013), Jhanwar and Jethwa (2000), and Bunnual and Naewbunthud (2012).

2. Theory and Experimental Blasting Drilling Pattern

2.1 Theory: Wavefront reinforcement of blast vibration

When a single blasthole is fired, a vibration wavefront occurs and spreads uniformly in all directions at the propagation of a seismic velocity, v_p . At any period after the blast, the wavefront will be at a radius r from the blasthole, which is proportional to time t in accordance with the relationship $r = v_p \times t$, as shown in Figure 1. When two blastholes are fired with a time delay between holes, the wavefronts will be of different radii because of the delay time and different centers, as shown in Figure 2. Under certain circumstances, when the distances between holes and the time delay period coincide with the travel time of the wavefront between blastholes, the wavefronts will coincide in one direction, as shown in Figure 3.

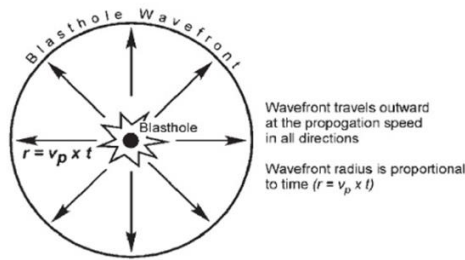


Figure 1. Wavefront propagation from blasthole (Richards, 2008).

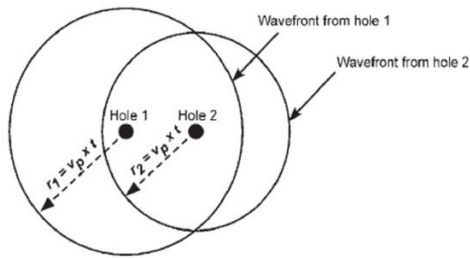


Figure 2. Wavefronts from two blastholes with time delay between initiations (Richards, 2008).

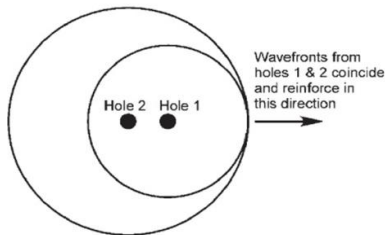


Figure 3. Reinforcing wavefronts from two blastholes with time delay between initiation (Richards, 2008).

2.2 Blasting drill pattern

Several drill patterns are used in blasting operations, depending on the contractor. The experimental blastings were monitored and recorded from overburden blastings, mainly in two pits at the Mae Moh Mine: Southeast pits (B3, B5) and Central pits (A6), as shown in Figure 4. Most blasting patterns used in the experimental blasts were staggered patterns – 10 blastholes per row with 4 rows, for a total of 40 blastholes per round. The delay number of each blasthole varied from No.1 to No.10 or 25 to 275 milliseconds delay. The blaster used a sequential timer blasting machine to separate 40 blastholes into 4 circuits, with 10 holes per circuit, with a 155 millisecond delay between each circuit or row. The delay time for each blast hole is also shown in Figure 5. The drill patterns of some experimental blasts differed. The 7-inch diameter blastholes were in a staggered pattern. Burden x spacing was 4x5 or 5x6 meters and a hole depth of 6 meters. Stemming, sub-drill, and charge length are 3.6, 0.5, and 2.4 meters, respectively, as shown in Figure 6.

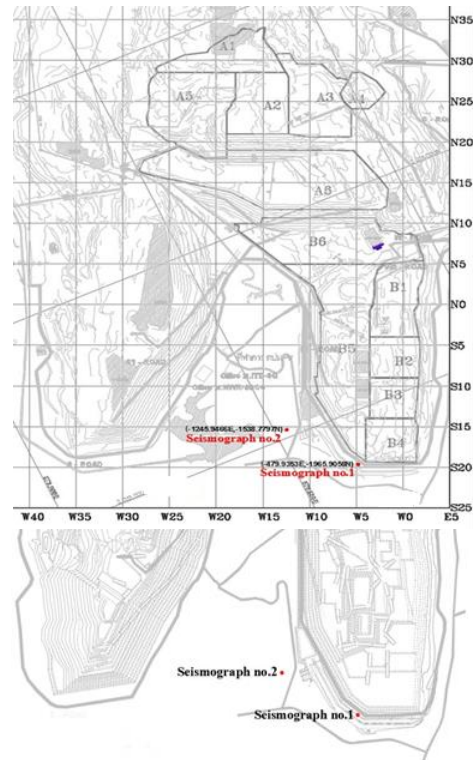


Figure 4. Details of the partial operating pits at Mae Moh Mine; Most experimental blastings were conducted in the South-East Pit (B3, B5) and two seismographs are located.

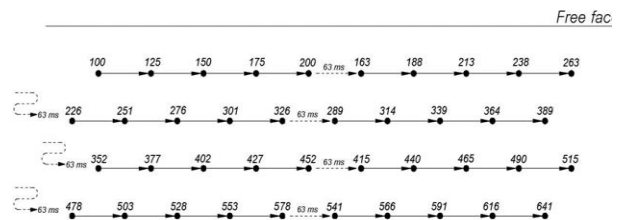


Figure 5. Example of drill patterns and delay time of the experimental blastings.

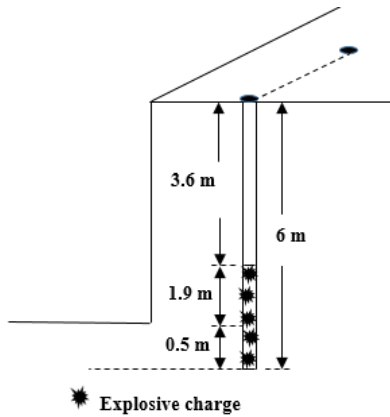


Figure 6. Blasthole geometry.

3. Methods

1. Collect the coordinates of blast holes and drill pattern, including the burden, spacing, and delay time between blast holes of the experimental blastings.
2. Record the coordinates of the first initiated blast hole as 0,0, and the remainder of the blast holes in relation to the first, in an Excel spreadsheet. Determine the radius of each blast hole from the predetermined wave velocity and time, as shown in Figure 7 (illustrated with $v_p = 2,000$ m/s and $t = 1,000$ ms).
3. Transfer only blast hole coordinates and radii data to a Scrip file in AutoCAD and use the command “circle X,Y, radius” in text format (.txt) and save file as scrip (.scr) that can be run in AutoCAD, as shown in Figure 8.
4. Use command scr in AutoCAD to run scrip for creating the wavefront circles from the first initiation blasthole to the last, as shown in Figure 9.
5. Move and rotate the wavefront circles to overlap the coordinates of the blast holes in the blasting area on the mine weekly operating map and identify the two locations – reinforcement and non-reinforcement of wavefront locations – that are equal distance, as shown in Figure 10. Use a handheld GPS to identify the reinforcement and non-reinforcement of wavefront locations and place seismographs at those locations. Record and analyze the vibrations from the blasting.

HoleNO.	DelayNO.	RowNO.	DelayTime	position		wavefront radius	Velocity
				x	y		atTime
1	2	0	50	0	0	2340.0	= 1200
2	4	0	100	5	0	2280.0	= 2000
3	6	0	150	10	0	2220.0	= 25
4	8	0	200	15	0	2160.0	delay between row = 155
5	10	0	250	20	0	2100.0	burden = 4
6	2	1	205	25	0	2154.0	spacing = 5
7	4	1	255	30	0	2094.0	
8	6	1	305	35	0	2034.0	
9	8	1	355	40	0	1974.0	
10	10	1	405	45	0	1914.0	
11	2	2	360	-2.5	-4	1968.0	
12	4	2	410	-2.5	-4	1908.0	
13	6	2	460	7.5	-4	1848.0	
14	8	2	510	12.5	-4	1788.0	
15	10	2	560	17.5	-4	1728.0	
16	2	3	515	22.5	-4	1782.0	
17	4	3	565	27.5	-4	1722.0	
18	6	3	615	32.5	-4	1662.0	
19	8	3	665	37.5	-4	1602.0	
20	10	3	715	42.5	-4	1542.0	
21	2	4	670	0	-8	1596.0	
22	4	4	720	5	-8	1536.0	
23	6	4	770	10	-8	1476.0	
24	8	4	820	15	-8	1416.0	

Figure 7. Blasthole coordinates and radii with drill pattern.

```

circle 0,0 2340.0
circle 5,0 2280.0
circle 10,0 2220.0
circle 15,0 2160.0
circle 20,0 2100.0
circle 25,0 2154.0
circle 30,0 2094.0
circle 35,0 2034.0
circle 40,0 1974.0
circle 45,0 1914.0
circle -2.5,-4 1968.0
circle 2.5,-4 1908.0
circle 7.5,-4 1848.0
circle 12.5,-4 1788.0
circle 17.5,-4 1728.0
circle 22.5,-4 1722.0
circle 27.5,-4 1722.0
circle 32.5,-4 1662.0
circle 37.5,-4 1602.0
circle 42.5,-4 1542.0
circle 0,-8 1596.0
circle 5,-8 1536.0
circle 10,-8 1476.0
circle 15,-8 1416.0
circle 20,-8 1356.0
circle 25,-8 1410.0
circle 30,-8 1350.0
circle 35,-8 1290.0
circle 40,-8 1230.0
circle 45,-8 1170.0
circle -2.5,-12 1224.0
circle 2.5,-12 1164.0
circle 7.5,-12 1104.0
circle 12.5,-12 1044.0
circle 17.5,-12 984.0
circle 22.5,-12 1038.0
circle 27.5,-12 978.0
circle 32.5,-12 918.0
circle 37.5,-12 858.0
circle 42.5,-12 798.0
circle 0,0 0.5
circle 5,0 0.5
circle 10,0 0.5
circle 15,0 0.5
circle 20,0 0.5
circle 25,0 0.5
circle 30,0 0.5
circle 35,0 0.5
circle 40,0 0.5
circle 45,0 0.5
circle -2.5,-4 0.5
circle 2.5,-4 0.5
circle 7.5,-4 0.5
circle 12.5,-4 0.5
circle 17.5,-4 0.5
circle 22.5,-4 0.5
circle 27.5,-4 0.5
circle 32.5,-4 0.5
circle 37.5,-4 0.5
circle 42.5,-4 0.5
circle 0,-8 0.5
    
```

Figure 8. Scrip file of blasthole coordinates and radii.

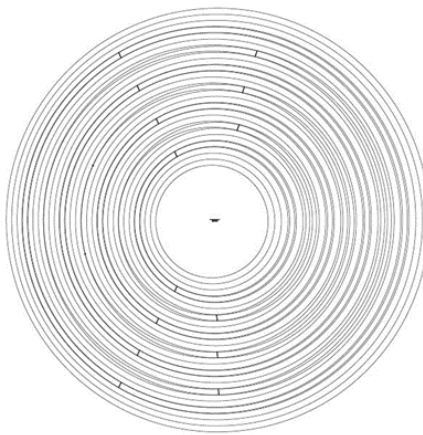


Figure 9. Wavefront circles generated from AutoCAD.

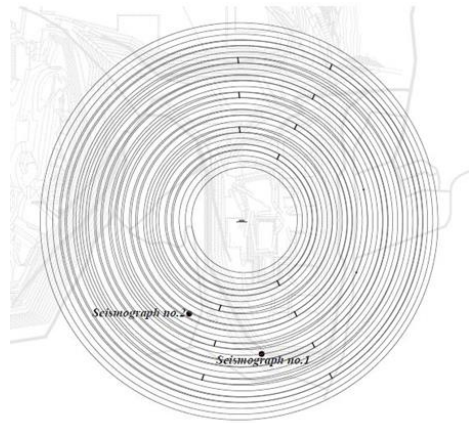


Figure 10. Overlapping wavefront circles on the map.

4. Results and Discussion

Twenty-one experimental blastings were conducted at Mae Moh Mine. The blastings were located in two main pits: South-East pit (B3, B5) and C-pit (A6). The distance of the two seismographs from the blasting area was less than 1,000 meters. The explosive charge per blasthole varied between 20-40 kilograms. The recorded peak particle velocities were less than 2 mm/s. The vector sum of the peak particle velocity (PVS) from each blast was considered, regardless of longitudinal, transverse, or vertical axis. The results of all 21 experimental blastings are shown in Table 1.

The drill patterns in the experimental blastings were staggered pattern and face blastings. Blasting sequence was

hole-by-hole using a sequential blasting machine. The delay time between holes was 25 milliseconds; however, the delay time of the circuits varied from 75-190 milliseconds, with 155 milliseconds the most common. The number of blast holes per round varied between 20-40 holes. The number of rows was limited to no more than 4 rows per round. The results from 21 test blasts on overburden material (the Red Beds) at various patterns and delay timing using a shear surface wave velocity of 350 m/s indicated that 16 of 21 test blasts (76%) showed the vector sum of peak particle velocities at the areas where the wavefront reinforcement occurred were higher than non-wavefront reinforcement areas. The rest 5 of 21 test blasts (24%) do not follow the wavefront reinforcement model probably caused by many extensional faults in the Mae Moh basin that have NW to SE direction and most are parallel to the boundary faults (Chatraprasert, 2005). The seismograph located behind any extensional fault mainly displays lower peak particle velocity (Sintuwong & Jaronpattanapong, 2011).

The seismic velocity used in this study was based on a study of shear surface waves by the Asian Institute of Technology (2009). The P or S seismic velocities were difficult to determine, because the important parameters – Young or Shear modulus – of the Red Bed have never been studied. From a preliminary study of the Red Bed material, the experiment was designed to use a shear surface wave V_{p30} of 350 m/s, based on the study from Asian Institute of Technology as above-mentioned. The positioning of the seismographs was for the most parts placed within the operating pits, at a distance of less than 1,000 meters from the blasting areas. Due to the amount of the explosives used, the seismographs could not detect the particle velocity beyond 1,500 meter.

Table 1. Results of the 21 experimental blastings.

Blast No.	Blast Direction	Descriptions										Explosive charge per hole (kg)	Pattern BxSxH (m)	Blasted material		
		Seismograph A				Reinforcement	Distance (m)	Seismograph B							Reinforcement	Distance (m)
		PPV (mm/s)		PVS (mm/s)				PPV (mm/s)		PVS (mm/s)						
T	V	L	(mm/s)	T	V	L	(mm/s)									
1	E	0.540	0.381	0.429	0.650	×	1,238.4	0.508	0.508	0.381	0.539	√	1,021.1	25	4 x 5 x 6	red bed
2	S	1.190	1.050	1.100	1.500	√	1,415.2	1.400	0.889	1.650	1.920	×	1,135.6	37.5	5 x 6 x 6	red bed
3	S	0.714	0.302	0.587	0.897	√	2,306.5	0.371	0.571	0.524	0.594	×	2,006.8	37.5	5 x 6 x 6	red bed
4	S	0.889	0.730	0.952	1.170	√	1,354.8	0.857	0.921	0.810	0.120	×	1,089.3	37.5	5 x 6 x 6	red bed
5	S	0.794	1.050	1.020	1.160	×	1,285.7	1.160	1.320	1.370	1.390	√	994.7	30	4.5 x 5.5 x 6	red bed
6	S	0.683	0.683	1.020	1.050	√	1,363.6	0.714	0.810	0.810	0.949	×	1,113.8	37.5	6 x 6 x 6	red bed
7	S	0.778	0.778	0.921	1.170	√	1,303.5	0.762	0.857	0.937	0.997	×	1,016.6	30	4.5 x 5.5 x 6	red bed
8	S46°E	4.860	5.790	9.380	9.640	√	576	1.030	1.130	0.984	1.210	×	560	37.5	5 x 6 x 6	red bed
9	S46°E	2.810	3.480	3.370	4.680	√	580	0.714	0.841	0.778	0.906	×	606	37.5	5 x 6 x 6	red bed
10	S68°E	2.030	1.860	2.030	2.570	×	1,179	0.825	1.100	0.762	1.230	√	943	25	4 x 5 x 5	red bed
11	S68°E	1.270	1.540	1.030	1.820	×	1,194	0.492	0.730	0.942	0.901	√	900	25	4 x 5 x 5	red bed
12	S52°E	0.841	1.440	1.190	1.700	√	698	0.481	1.020	0.587	1.120	×	702	25	4 x 5 x 6	red bed
13	S34°E	2.650	1.440	1.890	3.030	√	663	1.670	1.780	1.570	2.340	×	449	37.5	4 x 5 x 6	red bed
14	S60°E	1.330	1.350	1.220	1.690	√	664	1.110	0.905	0.619	1.240	×	650	37.5	5 x 6 x 6	red bed
15	S	1.400	1.950	1.760	2.350	√	712	1.270	1.300	1.100	1.720	×	691	30	3 x 5 x 6	red bed
16	S	1.710	1.400	0.079	1.720	×	710	6.450	3.970	4.290	7.670	√	721	45	5 x 6 x 6	red bed
17	S46°E	0.635	1.430	0.905	1.480	√	960	2.460	1.950	1.970	2.690	×	963	40	6 x 7 x 6	red bed
18	S52°E	1.340	1.030	0.968	1.510	√	960	0.619	0.889	0.683	0.912	×	963	40	6 x 7 x 6	red bed
19	S68°E	0.778	0.794	1.750	1.750	×	852	1.110	1.160	1.330	1.790	√	909	40	6 x 7 x 6	red bed
20	S60°E	1.270	1.110	1.330	2.120	√	858	0.429	0.286	0.635	0.674	×	797	40	6 x 7 x 6	red bed
21	S50°E	0.492	0.381	0.387	0.605	×	809	0.984	0.317	0.333	1.030	√	772	40	6 x 7 x 6	red bed

Note:1. / indicates that the seismograph was placed at the wavefront reinforcement location and x indicates that the seismograph was placed at the wavefront non-reinforcement location.2. Blast number 1, 2, 10, 11 and 17 indicate results that did not fit the wavefront reinforcement model.



Figure 11. BlastMate III Seismograph.

From the pattern and delay time used in the experimental blastings, the results indicated that the wavefront reinforcement mainly clustered in front and to the back of the blast direction, as shown in Figure 12. However, the wavefront reinforcement areas can occur to sides, if the delay timing is not designed properly – for example, the blasting sequence switches from one hole and cross over to another hole in the same row, rather than consecutive blasting. Changing the seismic velocity had little effect on the wavefront reinforcement direction. The circuit delay time between rows or circuits used in the experimental blastings varied from 63-163 milliseconds. Applying the wavefront reinforcement model, the recommended delay time between circuits or rows should be 200 milliseconds in order to decrease the reinforcement areas.

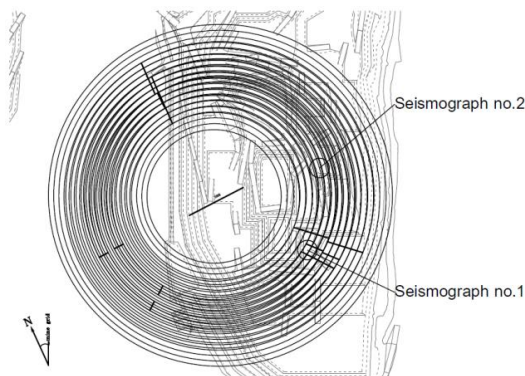


Figure 12. Straight lines indicate the wavefront reinforcement areas and directions mostly occur in front and to the back of the blast direction. In this figure (using experimental blasting number 13 as the example), the blast direction is to the Southeast.

The results from this study indicated that applying the wavefront reinforcement model can, with reasonable confidence, reduce the possibility of increasing ground vibrations from wavefront reinforcement by changing the blast direction.

5. Conclusions

The wavefront reinforcement model can be applied to identify the areas of wavefronts are reinforced by using drill

pattern and delay timing. In 16 of the 21 experimental blasts (76%) in this study, particle velocities at the areas where the wavefront reinforcement occurred were higher than at non-wavefront reinforcement areas. The wavefront reinforcement areas were generally clustered in two areas – in front and to the back of the blasting direction. Other wavefront reinforcement areas can occur to side of the blasting direction due to not having appropriate delay time between holes. The wavefront reinforcement model offers an alternative to reducing blast-induced ground vibrations.

Acknowledgements

The authors wish to sincerely acknowledge the full financial support provided by the Research Administration Center, Chiang Mai University. The authors are also grateful to all engineers and technicians at the Drilling and Blasting Section, Mae Moh Mine, the Electricity Generation Authority of Thailand (EGAT) for their kind assistance and support during the project.

References

- Boonnumma, A., & Leelasukseree, C. (2013). Induced seismic force reduction using air deck blasting at Mae Moh mine, Thailand. *Proceedings of the 47th US Rock Mechanics and Geomechanics Symposium 2013*, 13-297.
- Bunnual, P., & Naewbunthud, S. (2012). A study on air-deck blasting applied for limestone quarries. *Proceedings of the 10th International Conference on Mining, Materials and Petroleum Engineering*, Songkhla, Thailand.
- Chantraprasert, S. (2005). Evidence for inversion in the Mae Moh Basin, Northern Thailand. *Proceedings of the International Conference on Geology, Geotechnology and Mineral Resources of Indochina*, Khon Kaen, Thailand.
- Dogan, O., Anil, O., Akbas, S. O., Kantar, E., & Erdem, T. (2013). Evaluation of blast-induced ground vibration effects in a new residential zone. *Soil Dynamics and Earthquake Engineering*, 50(2013), 168-181.
- Geotechnical Report Mae Moh Mine. (1985). February 1985, Vol.3, E 14.
- Hasanipanah, M., Monjezi, M., Shahnazar, A., Armaghani, D. J., & Farazmand, A. (2015). Feasibility of indirect determination of blast induced ground vibration based on support vector machine. *Measurement*, 75, 289-297.
- Jhanwar, J. C., & Jethwa, J. L. (2000). The use of air decks in production blasting in an open pit coal mine. *Geotechnical and Geological Engineering*, 18, 269-287.
- Kahrman, A. (2004). Analysis of parameters of ground vibration produced from bench blasting at a limestone quarry. *Soil Dynamics and Earthquake Engineering*, 24(11), 887-892.
- Lheewijit, W., Bunnual, P., & Rachpech, V. (2012). A comparison study on conventional blasting and stem plug blasting technique. *Proceedings of the 10th International Conference on Mining, Materials and Petroleum Engineering*, Songkhla, Thailand.

- Mavong, N., Chaiwan, A., & Leelasukseree, C. (2014). A rock mass elastic modulus estimation using Mae Moh Mine's large scale experiment data. *Proceedings of EUROCK 2014. ISRM European Regional Symposium*, Vigo, Spain.
- Ozer, U., Kahrman, A., Aksoy, M., Adiguzel, D., & Karadogan, A. (2008). The analysis of ground vibrations induced by bench blasting at Akyol quarry and practical blasting charts. *Environmental Geology*, 54, 737-743.
- Rachpech, V., Bunnual, P., Julapong, P., & Walthongthanawut, T. (2014). Local ground parameters of blasting vibration model for different geological structure. *Songklanakarin Journal of Science and Technology*, 36(1), 89-95.
- Ratanasthien, B., Takashima, I., & Matsubaya, O. (2008). Paleogeography and Climatic Change Recorded on Viviparidae Carbon and Oxygen Isotope in Mae Moh Coal Mine, Northern Thailand. *Bulletin of the Geological Survey of Japan*, 59(7/8), 327-338.
- Richard, A. B. (2008). Blast vibration wavefront reinforcement model. *Mining Technology*, 117(4), 161-167.
- Shi, X. C., & Chen, S. R. (2011). Delay time optimization in blasting operations for mitigating the vibration-effects on final pit walls's stability. *Soil Dynamics and Earthquake Engineering*, 31, 1154-1158.
- Sintuwong, M., & Jaroonpattanapong, P. (2011). Modified scale distance for Mae Moh Mine. *Proceedings of the 9th National Conference on Mining, Materials and Petroleum Engineering*, Bangkok, Thailand.
- Songtham, W., Ugaib, H., Imsamuta, S., Maranateb, S., Tansathiena, W., Meesooka, A., & Saengsrichana, W. (2005). Middle miocene molluscan assemblages in Mae Moh Basin, Lampang Province, Northern Thailand. *Science Asia*, 31, 183-191.
- Yan, W. M., Tham, L. G., & Yuen, K. V. (2013). Reliability of empirical relation on the attenuation of blast-induced vibrations. *International Journal of Rock Mechanics and Mining Sciences*, 59(2013), 160-165.